Наносистеми, наноматеріали, нанотехнології
Nanosistemi, Nanomateriali, Nanotehnologii
2023, т. 21, № 1, сс. 199–208

PACS numbers: 68.37.Vj, 81.07.Pr, 81.16.-c, 87.19.xb, 87.64.Ee, 87.64.M-, 87.85.Rs

Preparation, Morphological and Antibacterial Activity of PS–PC/MnO_2–SiC Nanocomposites for Biomedical Applications

Mohanad H. Meteab, Ahmed Hashim, and Bahaa H. Rabee

College of Education for Pure Sciences,
Department of Physics,
University of Babylon,
Hillah, Iraq

In this work, nanostructures of polystyrene (PS), polycarbonate (PC), manganese-dioxide nanoparticles (MnO_2 NPs), and silicon carbide nanoparticles (SiC NPs) are fabricated to use as coating materials for antibacterial applications. The casting method is used to make nanocomposites' films made of PS–PC/MnO_2–SiC. The field emission scanning electron microscopy (FE-SEM), optical microscopy (OM), and antibacterial activity are tested. Analysis with FE-SEM and OM shows that the MnO_2/SiC NPs are spread out evenly in the polymeric matrix. The diameters of the inhibition zones for gram-negative bacteria (*Salmonella*) are bigger than the diameters of the inhibition zones for gram-positive bacteria (*S.aureus*). This means that the prepared nanocomposites work better with gram-negative bacteria than with gram-positive bacteria and, therefore, have potential applications in biotechnology and biomedical science.

Наноструктури полістиролу (ПС), полікарбонату (ПК), наночастинок діоксиду Манґану (MnO_2-НЧ) та наночастинок карбіду Силіцію (SiC-НЧ) виготовлено для використання в якості матеріялів покриття для антибактеріяльних застосувань. Метод лиття використовується для виготовлення плівок нанокомпозитів з ПС–ПК/MnO_2–SiC. Тестуються польова емісійна сканувальна електронна мікроскопія (ПЕ-СЕМ), оптична мікроскопія (ОМ) та антибактеріяльна активність. Аналіза за допомогою ПЕ-СЕМ і ОМ показує, що MnO_2/SiC-НЧ рівномірно розподілені у полімерній матриці. Діяметри зон інгібування грамнеґативних бактерій (*Salmonella*) більші, ніж діяметри зон інгібування для грампозитивних бактерій (*S.aureus*). Це означає, що підготовлені нанокомпозити ліпше працюють з грамнеґативними бактеріями, ніж з грампозитивними, і мають потенційне застосування в біотехнології та біомедичній науці.

Key words: silicon carbide, manganese dioxide, polystyrene, polycarbonate, field emission scanning electron microscopy, optical microscopy,

antibacterial applications, reactive oxygen species.

Ключові слова: карбід Силіцію, діоксид Манґану, полістирол, полікарбонат, польова емісійна сканувальна електронна мікроскопія, оптична мікроскопія, антибактеріяльні аплікації, активні форми кисню.

(Received 25 June, 2022)

1. INTRODUCTION

Microorganisms' contamination is a key factor in many areas, such as medical devices, dental equipment, healthcare products and hygienic applications, hospital surfaces and furniture, dental restoration, water purification systems, food packaging and storage, and so on. To solve this problem, different ways of sterilizing and antisepsis are used on different types of thermoplastic materials, such as dry or wet heating and ionic radiation. However, when these polymers are in the environment, microorganisms can make them dirty. Because of this, it is very important to find new polymeric materials that kill bacteria. Thermoplastics are strong and can stand up to being sterilized over and over, as well as high temperatures and harsh chemicals. So, antimicrobial polymer composites can be used as a way to avoid hospital-acquired infections. They can be made by adding a biocide agent to the bulk of the polymer, while it is being made or by coating the surface [1].

Polystyrene (PS) is one of the most common thermoplastic polymers used in many industries, such as food packaging. Due to its high stiffness, strength, durability, good thermal properties, low moisture absorption, transparency, light density, ease of processing and moulding, and low cost, this polymer is often used to package food [2–4].

Polycarbonate (PC) is a thermoplastic polymer that is used in a number of engineering fields, such as the car industry, data storage, and building. Due to its softness, notch sensitivity of mechanical properties, and high melt viscosity, it is not good for advanced applications. To improve its properties, it is mixed with other thermoplastic polymers or organic and inorganic additives like nanoalumina, graphene, and multi wall nanotubes [5].

MnO_2 NPs have a strong and broad optical absorption spectrum, which makes them a high-efficiency, wide-spectrum fluorescence quencher for the design of fluorescence opening probes to measure transmission potency [6]. In addition, intracellular glutathione can turn MnO_2 NPs into Mn^{2+}, which can be monitored using activated magnetic resonance and fluorescence signals [7, 8]. Manganese is also an important part of the human body, and its metabolism does not cause a serious immune response. Even though MnO_2-based na-

nomedical applications are getting better, it is not much known yet about how MnO_2 nanosheets might affect bacteria [8].

The goals of this study were to look into MnO_2 NPs ability to kill *Salmonella* in a lab setting for the first time and figure out how they interact with *Salmonella*. *Salmonella*, which is a major cause of food-borne disease outbreaks, is still a big problem in the poultry industry and in public health. To fight *Salmonella*, it is important to find new ways to do things and new ways to make drugs. We made MnO_2 nanosheets by treating them with ultrasonic waves at room temperature. Then, we used *Salmonella* as a model pathogen to study how well they kill bacteria. Our results suggest that MnO_2 nanosheets kill bacteria very well and could be used instead of or in addition to antibiotics to stop pathogens from getting into food [9].

Silicon carbide (SiC) was one of many one-dimensional nanomaterials that were strong, chemically stable, and resistant to bacteria. In addition, nanomaterials made of single-crystalline SiC were very good at killing bacteria. SiC nanowires (NWs) are more antibacterial than nanobelts, which have a lower density of stacking faults (SFs) and a 3C-structure twin domain with no flaws. By the surface polarity and free energy, SiC NWs have a lot of twins and/or SFs [10]. Overusing traditional antibiotics has led to new strains of bacteria that are becoming more resistant, which could be bad for public health. Scientists from many different fields have tried to come up with solutions that might help to solve this problem. In this situation, making new materials that kill bacteria has become an important and current goal in the field of materials science [11].

The present work aims to fabrication of PS–PC/MnO_2–SiC nanocomposites and studying their structure and antibacterial properties so that they can be used as coating materials for antibacterial applications.

2. MATERIALS AND METHODS

Polystyrene (PS)/polycarbonate (PC) films were mixed with manganese dioxide nanoparticles (MnO_2 NPs) with a purity of 98% and a size of 50 nm, and silicon carbide nanoparticles (SiC NPs) with a purity of 99% and a size of 80 nm. The 50/50 blend film was made by dissolving 1 g of each of these polymers in distilled chloroform (50 ml). The nanocomposites films were made by adding MnO_2 NPs and SiC NPs to a solution (PS/PC) with ratios (1.3%, 2.6%, 3.9% and 5.2%).

The field emission scanning electron microscopy (FE-SEM), the optical microscopy (OM), and antibacterial applications of PS–PC/MnO_2–SiC nanocomposites were investigated.

The antibacterial was determined using a disc diffusion method. PS–PC/MnO_2–SiC nanocomposite was used. When the ratio of diameter of inhibition is taken from the diameters of bacterial inhibition for

the sample that killed the most bacteria compared to the sample that did not kill the bacteria, the following equation was used to figure out the overlapping respiratory inhibition ratios of bacteria [12]:

$$R_{D(inhibition)}\% = (D_{inhibition} - D_{uninhibition})/D_{inhibition} \cdot 100\%, \qquad (1)$$

where $R_{D(inhibition)}\%$ is the percentage increase in the diameter of the inhibition zone of the bacterial respiratory overexpression inhibition zone after adding the nanocomposite, $D_{inhibition}$ is the diameter of the inhibition zone of the sample, where bacteria were killed, and $D_{uninhibition}$ is the diameter of the inhibition zones of the sample, where no bacteria were killed.

3. RESULTS AND DISCUSSION

Figure 1 represents the geometric structures of the PS/PC blends (51 atoms), while the optimized structures of the PS–PC/MnO_2–SiC nanocomposites (56 atoms) are obtained in Fig. 2.

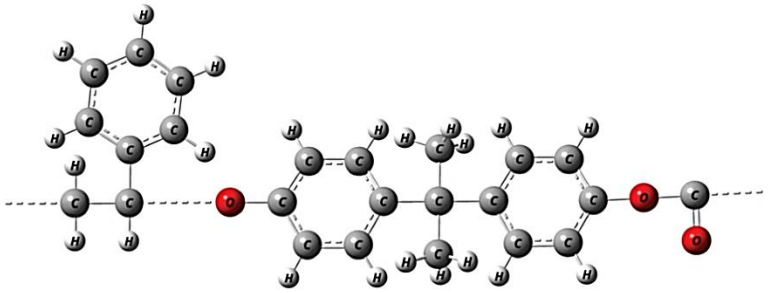

Fig. 1. Optimization of the geometries of PS–PC blends (51 atoms).

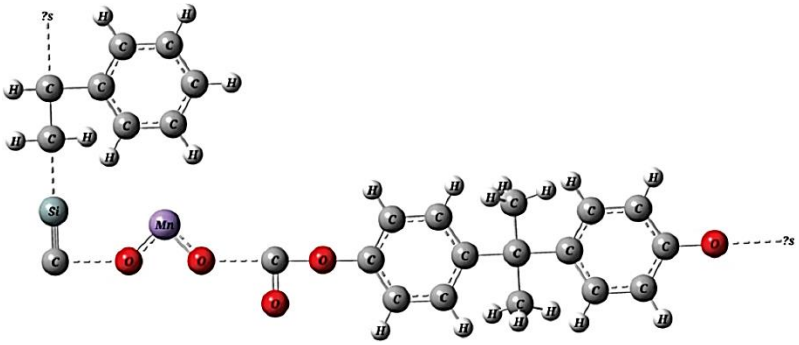

Fig. 2. The optimized structures of the PS–PC/MnO_2–SiC nanocomposites (56 atoms).

Figures 3 and 4 represent the field emission scanning electron microscopy (FE-SEM) and photomicrograph images (OM) of PS/PC blends with varying concentrations of MnO_2/SiC nanoparticles are depicted. Clusters of nanoparticles form at lower concentrations, as depicted in these images. With an increase in the content of nanoparticles in the matrix, a network is formed [13–18]. The surface morphology of the nanocomposites (PS–PC/MnO_2–SiC) has changed significantly as a result of the nanoparticle addition.

The photos show that the grains grow as the nanoparticle fraction rises. There are several randomly distributed aggregates or particles on the upper surface of the films made of nanocomposites (PS–PC/MnO_2–SiC). The number of white dots on the surface increases as the MnO_2/SiC-nanoparticle concentration increases. Grain

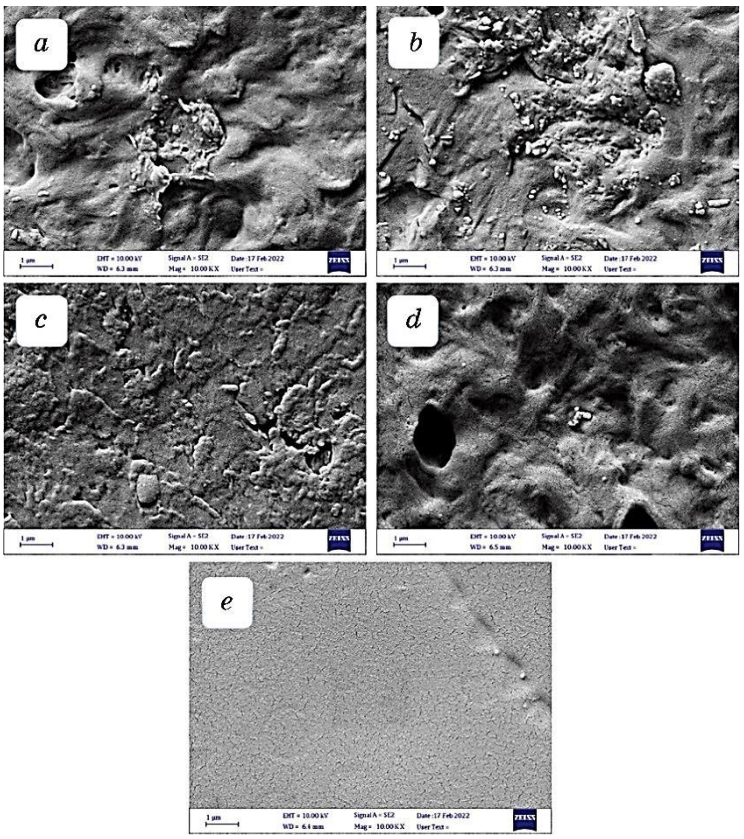

Fig. 3. FE-SEM micrographs (1-micro) of PS–PC/MnO_2–SiC nanocomposites: (*a*) for pure; (*b*) for 1.3 wt.% MnO_2/SiC NPs; (*c*) for 2.6 wt.% MnO_2/SiC NPs; (*d*) for 3.9 wt.% MnO_2/SiC NPs; (*e*) for 5.2 wt.% MnO_2/Si) NPs.

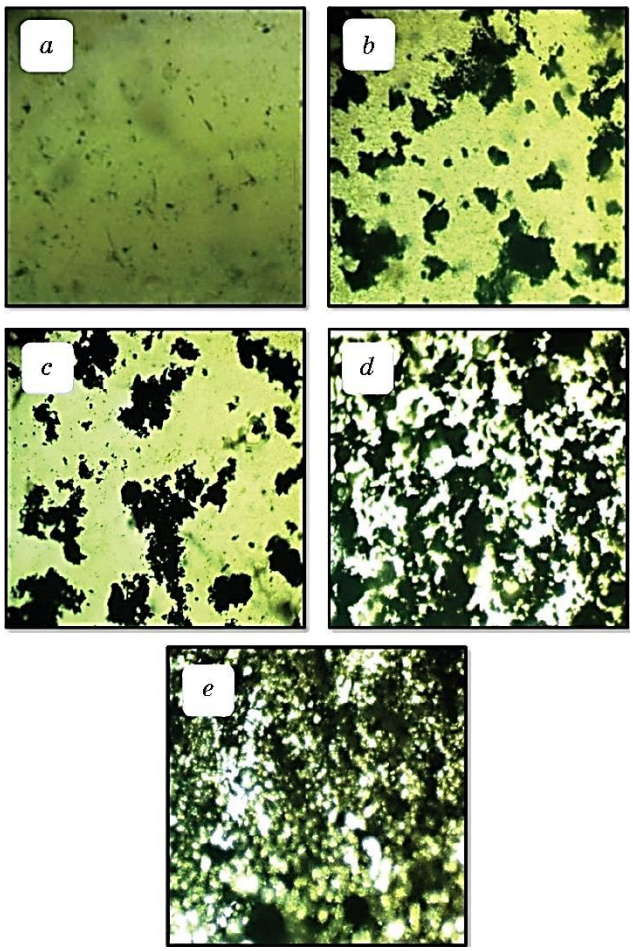

Fig. 4. Photomicrographs (×10) for PS–PC/MnO_2–SiC nanocomposites: (*a*) for pure; (*b*) for 1.3 wt.% MnO_2/SiC NPs; (*c*) for 2.6 wt.% MnO_2/SiC NPs; (*d*) for 3.9 wt.% MnO_2/SiC NPs; (*e*) for 5.2 wt.% MnO_2/SiC NPs.

distribution on the films' surfaces is uniformly dense. In polymer matrix, nanoparticles tend to form well-distributed aggregates. The MnO_2/SiC nanoparticles are found to be randomly dispersed in PS/PC matrix, and it is assumed that small agglomerates are generated in these films.

Antibacterial effects were investigated using inhibition of microbial biofilm made from PS–PC/MnO_2–SiC nanocomposites with varying weight percentages (1.3, 2.6, 3.9 and 5.2 wt.%).

For gram-positive bacteria (*Staphylococcus aureus*) and gram-negative bacteria (*Salmonella*), the antibacterial activity was measured by measuring the dimeters of inhibition around each sample

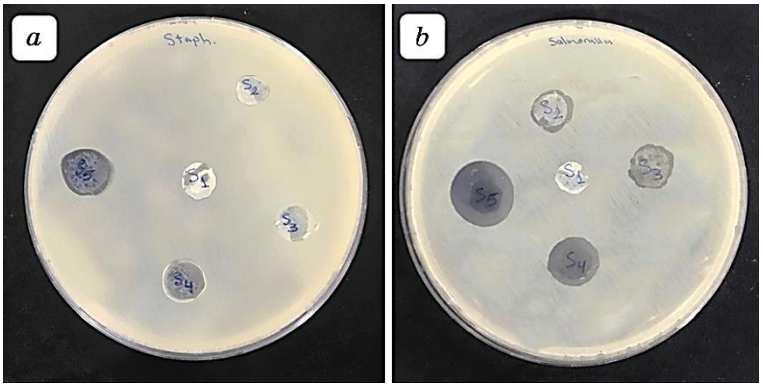

Fig. 5. Antibacterial activity of PS–PC/MnO_2–SiC nanocomposite: (*a*) images for inhibition zone of gram-positive bacteria; (*b*) images for inhibition zone of gram-negative bacteria against *Staphylococcus aureus* and *Salmonella*.

TABLE. The values of inhibition zone diameter of PS–PC/MnO_2–SiC nanocomposites.

Content of MnO_2, SiC NPs [wt.%]	Inhibition zone diameter	
	gram-positive (*Staphylococcus aureus*)	gram-negative (*Salmonella*)
0	0	0
1.3	0	17
2.6	0	17
3.9	16	20
5.2	18	26

using the agar diffusion method, and they are calculated by using relation (1) as of about 28% and 47%, respectively, when the MnO_2/SiC NPs content reached at 5.2 wt.%.

Figure 5 shows that the gram-negative (*Salmonella*) inhibited NPs' films more effectively than the gram-positive drug (*Staphylococcus aureus*). Inhibition zone diameter increases with increasing MnO_2/SiC NPs content.

Nanocomposites' ability to inhibit microorganisms is seen in Table.

As demonstrated in Figs. 6 and 7, increasing the concentration of nanoparticles results in an increase in inhibition. Antibacterial action has been linked to reactive oxygen species (ROS) inhibition because of their ability to degrade bacterial cell membranes, as well as their influence on ROS levels [19–23].

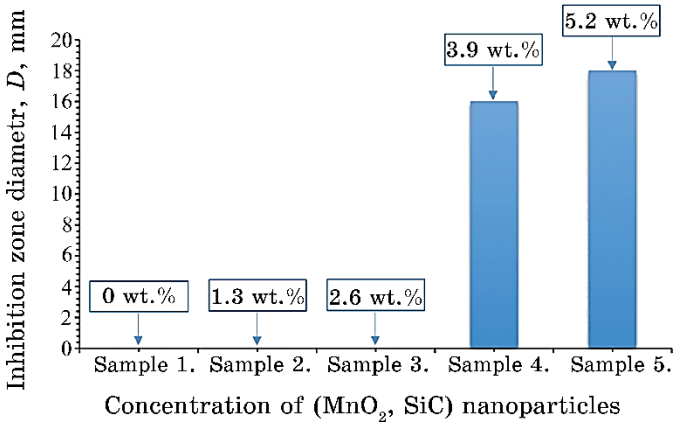

Fig. 6. Inhibition zone diameter of PS–PC/MnO_2–SiC nanocomposites for gram-positive bacteria (*Staphylococcus aureus*) with concentration (pure polymer blends, 1.3 wt.%, 2.6 wt.%, 3.9 wt.% and 5.2 wt.%).

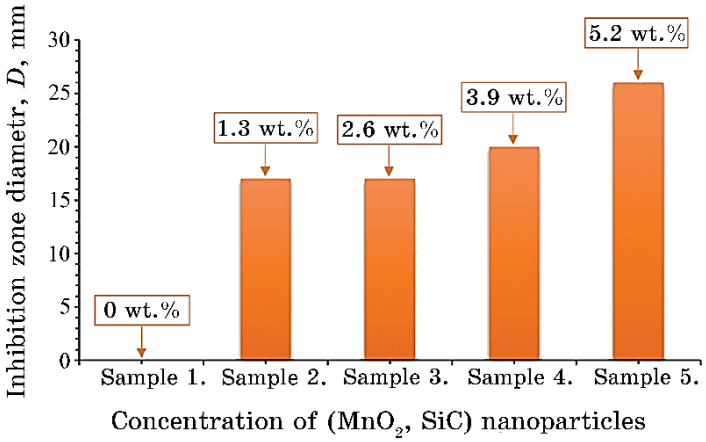

Fig. 7. Inhibition zone diameter of (PS–PC/MnO_2–SiC) nanocomposites for gram-negative bacteria (*Salmonella*) with concentration (pure polymer blends, 1.3 wt.%, 2.6 wt.%, 3.9 wt.% and 5.2 wt.%).

4. CONCLUSIONS

This work includes enhancing the structural and antibacterial activity of the PS–PC/MnO_2–SiC nanocomposites. Optical microscopy showed that as the nanomaterial concentration goes up, it forms a network inside the superimposed layer, which is a way for charge to move. The FE-SEM results showed that the NPs on the surface of the polymeric mixture was spread out evenly and that adding the

filler material made spherical clumps appear. The results of the antibacterial activity showed that the diameter of inhibition for gram-negative bacteria was larger than the diameter of inhibition for gram-positive bacteria. The final results exhibit that the PS–PC/MnO_2–SiC nanocomposites can be said that making these hybrid materials could be useful in a many of biotechnology and medical engineering fields, such as medical devices, antibacterial coatings, and biosensors.

REFERENCES

1. A. M. Díez-Pascual and J. A. Luceco-Sánchez, *Polym.*, **13**: 2105 (2021); https://doi.org/10.3390/polym13132105
2. A. E.Giannakas, C. E.Salmas, A. Karydis-Messinis, D. Moschovas, E. Kollia, V. Tsigkou, C. Proestos, A. Avgeropoulos, and N. E. Zafeiropoulos, *Appl. S.*, **11**: 9364 (2021); https://doi.org/10.3390/app11209364
3. L. A. Fakhri, B. Ghanbarzadeh, J. Dehghannya, F. Abbasi, and H. Ranjbar, *Food Packaging and Shelf Life*, **17**: 11 (2018); https://doi.org/10.1016/j.fpsl.2018.04.005
4. D. Hassan and A. Hashim, *J. Bionanosci.*, **12**: 341 (2018); https://doi.org/10.1166/jbns.2018.1533
5. N. Vidakis, M. Petousis, S. Grammatikos, V. Papadakis, A. Korlos, and N. Mountakis, *J. Nanomater.*, **12**: 1068 (2022); https://doi.org/10.3390/nano12071068
6. H. Fan, Z. Zhao, G. Yan, X. Zhang, C. Yang, H. Meng, Z. Chen, H. Liu, and W. Tan, *Angew. Chem. Int. Edit.*, **54**: 4801 (2015); https://doi.org/10.1002/ange.201411417
7. Z. Zhao, H. Fan, G. Zhou, H. Bai, H. Liang, R. Wang, X. Zhang, and W. Tan, *J. Am. Chem. Soc.*, **136**: 11220 (2014); https://doi.org/10.1021/ja5029364
8. J. Zhang, M. Xu, Y. Mu, J. Li, M. F. Foda, W. Zhang, K. Han, and H. Han, *J. Adv. Biomat.*, **218**: 119312 (2019); https://doi.org/10.1016/j.biomaterials.2019.119312
9. T. Du, S. Chen, J. Zhang, T. Li, P. Li, J. Liu, X. Du, and S. Wang, *J. Nanomater.*, **10**: 1545 (2020); https://doi.org/10.3390/nano10081545
10. M. S. Selim, P. J. Mo, Z. Hao, N. A. Fatthallah, and X. Chen, *J. Colloid Interf. Sci.*, **578**: 698 (2020); https://doi.org/10.1016/j.jcis.2020.06.058
11. J. R. Morones, J. L. Elechiguerra, A. Camacho, K. Holt, J. B. Kouri, J. T. Ramírez, and M. J. Yacaman, *Nanotechno.*, **16**, No. 10: 2346 (2005); https://doi.org/10.1088/0957-4484/16/10/059
12. G. Tong, M. Yulong, G. Peng, and X. Zirong, *Vet. Microbiol.*, **105**: 113 (2005); https://doi.org/10.1016/j.vetmic.2004.11.003
13. H. Abduljalil, A. Hashim, and A. Jewad, *European Journal of Scientific Research*, **63**, No. 2: 231 (2011).
14. A. Hashim, *Journal of Inorganic and Organometallic Polymers and Materials*, **31**: 2483 (2021); https://doi.org/10.1007/s10904-020-01846-6
15. A. Hashim, *J. Mater. Sci.: Mater. Electron.*, **32**: 2796 (2021); https://doi.org/10.1007/s10854-020-05032-9

16. A. Hashim and Z. S. Hamad, *J. of Bionanoscience*, **12**, No. 4: 488 (2018); doi:10.1166/jbns.2018.1551
17. A. Hashim and Q. Hadi, *Sensor Letters*, **15**, No. 11: 951 (2017); doi:10.1166/sl.2017.3892
18. B. Hussien, A. Hashim, and A. Jewad, *European Journal of Social Sciences*, **32**, No. 2: 225 (2012).
19. A. Hashim, H. M. Abduljalil, and H. Ahmed, *Egypt. J. Chem.*, **63**, No. 1: 71 (2020); doi:10.21608/EJCHEM.2019.10712.1695
20. H. Ahmed, A. Hashim, and H. M. Abduljalil, *Egypt. J. Chem.*, **62**, No. 4: 1167 (2019); doi:10.21608/EJCHEM.2019.6241.1522
21. A. Hashim, I. R. Agool, and K. J. Kadhim, *J. of Bionanoscience*, **12**, No. 5: 608 (2018); doi:10.1166/jbns.2018.1580
22. A. Hazim, A. Hashim, and H. M. Abduljalil, *Int. J. of Emerging Trends in Engineering Research*, **7**, No. 8: 68 (2019); https://doi.org/10.30534/ijeter/2019/01782019
23. A. Hazim, H. M. Abduljalil, and A. Hashim, *Int. J. of Emerging Trends in Engineering Research*, **7**, No. 8: 104 (2019); https://doi.org/10.30534/ijeter/2019/04782019